



LETTER OPEN

A bacteria-based system expressing anti-TNF- α nanobody for enhanced cancer immunotherapy

Signal Transduction and Targeted Therapy (2023)8:134

; <https://doi.org/10.1038/s41392-023-01364-0>

Dear Editor,

As a successful drug for inflammatory diseases, the application of TNF- α inhibitor on cancer therapy is limited by repeated administration and off-target effects.¹ A body of evidence indicated that the anti-tumor efficacy of TNF- α inhibitor is unsatisfactory, though repeated administration was used to improve its efficacy in tumor-treating fields, it will also lead to severe side effects and high cost.^{2–4} Hence, an efficient and highly targeted TNF- α antibody delivery system is worth developing.

The genetically modified strain of attenuated *Salmonella typhimurium* VNP20009 (VNP) not only has super tumor-targeting capacity and genetic stability in vivo, but also has thousands of times higher enrichment in tumors than that of liver and spleen.⁵ Thus, in this work, we built a novel VNP delivery system expressing anti-TNF- α nanobody (VNP _{α TNF- α}) (Fig. 1a and Supplementary Fig. S1a–g), which could significantly improve the delivery efficiency by continuous release of the nanobody under a hypoxic tumor environment (Fig. 1b and Supplementary Fig. S2a–d). Moreover, another strain of VNP _{α TNF- α /mCherry} was constructed with TNF- α nb fused to mCherry for the visualization of expressed TNF- α nb (Supplementary Fig. S1h–j). The TNF- α nb secreted by VNP had a similar particle size (75.27 ± 14.08 nm) and affinity compared with pure nanobody synthesized in our previous work⁶ (Supplementary Fig. S2e, f). VNP _{α TNF- α} induced about 40% apoptosis of B16F10 which was similar to that of VNP, while pure TNF- α nb couldn't induce cell apoptosis, the results confirmed the antitumor activity of VNP and VNP _{α TNF- α} in vitro (Supplementary Fig. S3b, c). In addition, VNP _{α TNF- α} stimulated dendritic cells (DCs) activation and cytotoxic CD8⁺ T cell production in vitro (Fig. 1c, d). VNP _{α TNF- α} stimulated CD8⁺ T cell production immediately by activating macrophage antigen presentation (Fig. 1e, Supplementary Fig. S3d). To evaluate the neutralization ability of VNP _{α TNF- α} , the supernatants of M1-type RAW264.7 were collected to measure the level of TNF- α . The result indicated that VNP _{α TNF- α} treatment significantly neutralized secreted TNF- α (sTNF- α), thus, decreasing the level of sTNF- α (Supplementary Fig. S3e).

To evaluate the tumor targeting ability of VNP _{α TNF- α} , the organ burdens of bacteria were measured (Supplementary Fig. S4a). It was indicated that both VNP and VNP _{α TNF- α} showed tumor targeting ability as expected, which were hundreds to thousands of times higher than other tissue (Fig. 1f, Supplementary Fig. S4c). To further study the tumor residence time of TNF- α nb in tumor, we injected TNF- α nb-mCherry (150 μ g/kg) and VNP _{α TNF- α /mCherry} (1×10^8 CFU, the amount of secreted TNF- α nb-mCherry was equivalent to that of TNF- α nb-mCherry group) according to our data. At first, the MFI of TNF- α nb-mCherry in tumor tissue was 1.3 times higher than that of VNP _{α TNF- α /mCherry} within 4 hours. After 12 hours, pure TNF- α nb was depleted slowly, while TNF- α nb-mCherry of VNP _{α TNF- α /mCherry} increased to 2.3 times higher than pure TNF- α nb as VNP proliferated continuously (Fig. 1g, Supplementary Fig. S4b).

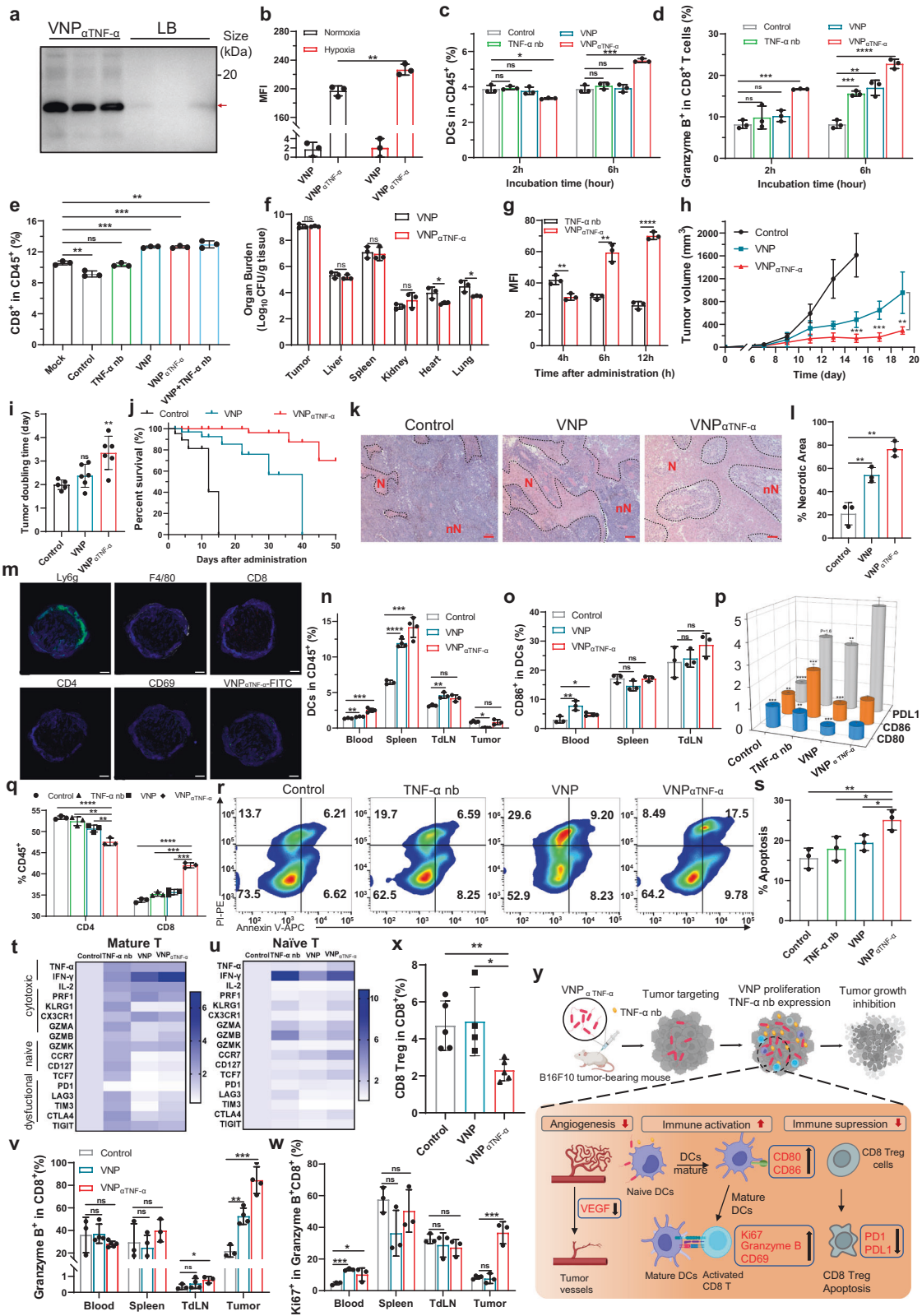
Next, the antitumor effect of VNP _{α TNF- α} in vivo was evaluated (Supplementary Fig. S5a). The tumor growth curve indicated that VNP _{α TNF- α} effectively inhibited melanoma progression (Fig. 1h). In addition, delayed tumor doubling time (TDT) was 2.38 days in the VNP group and 3.35 days in the VNP _{α TNF- α} group, and the TDT ratio of VNP _{α TNF- α} to PBS or VNP reached 1.67 times or 1.4 times respectively (Fig. 1i). VNP _{α TNF- α} also prolonged tumor-bearing mouse survival significantly than that of VNP (Fig. 1j). These results suggested that VNP _{α TNF- α} had an excellent therapeutic effect. Moreover, the H&E analysis of tumor section showed that more than 75% of the tumor was necrotic after VNP _{α TNF- α} treatment (Fig. 1k, l). Next, we preliminarily explored the therapeutic mechanism of VNP _{α TNF- α} . Firstly, it is indicated that the level of transmembrane TNF- α (tmTNF- α) in VNP _{α TNF- α} was reduced, which is lower than the baseline of the PBS group (Supplementary Fig. S6a). Since it is reported that low-dose TNF- α induces angiogenesis while high-dose TNF- α lead to thrombosis within tumor vasculature,⁷ we then assessed the distribution and gene expression of tumor vessel by CD31 and vascular endothelial growth factor (VEGF) staining. It is shown in Supplementary Fig. S6b, c that VEGF and CD31 was downregulated in the VNP _{α TNF- α} group, suggesting that VNP _{α TNF- α} inhibited tumor progression by reducing the density of tumor vessels. Therefore, VNP _{α TNF- α} induced more cell apoptosis in the tumor tissue (Supplementary Fig. S6d).

To further elucidate the therapeutic mechanisms, the distribution of tumor-infiltrating immune cells was detected. The proportion of CD8⁺ T cells and CD69⁺ cells were significantly increased, approximately 11 and 7%, while the ratio of CD4⁺ T cells were reduced in the VNP _{α TNF- α} group (Fig. 1m). In addition, the proportions of neutrophils and macrophages were significantly increased both in the VNP and VNP _{α TNF- α} group (Fig. 1m, Supplementary Fig. S7a). Next, the proportion and state of DCs in vivo were investigated. It is shown that the ratio of DCs and activated DCs (CD86⁺DCs) were significantly increased in immune organs (Fig. 1n, o). The results were consistent with in vitro experiment, where VNP _{α TNF- α} induced the upregulation expression of CD86, CD80, and PDL1 of DC2.4 cells in vitro (Fig. 1p). As for in vivo experiment, the elevated level of CD86 and CD80, and the decrease level of PD1 and PDL1 in the tumor mixed pool were observed (Supplementary Fig. S5b). In addition, CD11b⁺ in DCs was upregulated 1.6 times higher than that of VNP in tumor, which means DCs were activated by VNP _{α TNF- α} (Supplementary Fig. S5c). Together, these results indicated that VNP _{α TNF- α} stimulated transformation from “cold” tumor with immune suppression to “hot” tumor with anti-tumor immune activation.

We further investigated whether VNP _{α TNF- α} could stimulate CD8⁺ T cell activation. Therefore, we firstly stimulated splenic T cells in vitro and cocultured them with B16F10-OVA cells as illustrated in Supplementary Fig. S5d, the cells in lower chambers were collected and tumor cell-recruited CD8⁺ T cells and B16F10-OVA cells apoptosis were analyzed. The results revealed that the

Received: 15 August 2022 Revised: 9 January 2023 Accepted: 12 February 2023

Published online: 19 April 2023



highest proportion of CD45⁺ cells in the lower chamber was T cells, which was approximately 90%, and the proportion of CD8⁺ T cells increased from 32 to 40%, in contrast, CD4⁺ T cells decreased after VNP_αTNF- α incubation (Fig. 1q), which indicated that VNP_αTNF- α stimulated CD8⁺ T cell chemotaxis and activation.

As a result, significant tumor apoptosis was induced from 15 to 25% by VNP_αTNF- α -stimulated splenic T cells (Fig. 1r, s). Further detection of relative expression of markers by RT-PCR showed that VNP_αTNF- α induced CD8⁺ T cell polarization into cytotoxic T cells, according to the upregulated *TNF- α* , *IFN- γ* , *IL-2*, *perforin*, and

Fig. 1 **a** The TNF- α nb expression inside bacteria or secreted into LB was detected by western blot ($n = 3$). **b** Expression of TNF- α nb-mCherry under normoxic and hypoxic (1% O₂) conditions ($n = 3$). **c** Ratio of splenic DCs after incubated with different groups for 2 h or 6 h ($n = 3$). **d** Proportion of granzyme B⁺CD8⁺ T cells after incubated with different groups for 2 h or 6 h ($n = 3$). **e** Counted CD8⁺ T cell ratio in splenic lymphocytes after RAW264.7 cells incubation ($n = 3$). **f** The organ burden of tumor-bearing mice 5 days after injection ($n = 3$). **g** MFI analysis of representative fluorescent image of colonized VNP _{α TNF- α /mCherry} (Red; 1×10^8 CFU/mouse) and TNF- α nb-mCherry (Red; 150 μ g/kg) in tumors ($n = 3$). **h** Tumor growth curves of B16F10 administered with PBS, VNP, or VNP _{α TNF- α} ($n = 6$). **i** The calculated tumor doubling time of different groups ($n = 6$). **j** Overall survival of the tumor-bearing mice ($n = 6$). **k, l** H&E staining of tumors after VNP _{α TNF- α} treatments. Scale bar, 200 μ m. N: necrotic region, nN: nonnecrotic region. **m** The distribution of tumor-infiltrating immune cells after VNP _{α TNF- α} administration. 1000 μ m scale bars shown. (Neutrophil: Ly6g⁺; Macrophage: F4/80⁺; CD8⁺; CD4⁺; active T cells: CD69⁺; VNP _{α TNF- α} : FITC⁺) **n** Quantification of DC cells in tumor and other related immune organs by flow cytometry (peripheral blood, spleen, and TdLNs) of tumor-bearing mice ($n = 4$). **o** Ratio of CD86⁺ in DCs ($n = 4$). **p** Expression of CD80, CD86, and PDL1 in DC2.4 cells after VNP _{α TNF- α} treatment ($n = 3$). **q** Ratio of CD8⁺ and CD4⁺ T cells in the lower chambers ($n = 3$). **r, s** Apoptosis ratio of B16F10-OVA cells after VNP _{α TNF- α} -stimulated splenocyte treatments ($n = 3$). **t, u** Collected unstimulated splenocytes (naïve T) and splenocytes activated by cytokine (mature T) and identified splenic T cells as naïve T cells, cytotoxic T cells, or dysfunctional T cells by RT-PCR. The bar is the relative expression level ($n = 3$). **v** Quantification of granzyme B⁺ CD8⁺ T cells in blood, spleen, TdLNs and tumor ($n = 4$). **w** Quantification of Ki67⁺ granzyme B⁺ CD8⁺ T cells in blood, spleen, TdLNs and tumor ($n = 4$). **x** Flow cytometry assessment of CD8 Treg cells by CD25 and CD122 markers ($n = 5$). **y** Schematic diagram of therapeutic mechanisms of B16F10-bearing mice by VNP _{α TNF- α} . Illustrations was made with BioRender. Data are shown as the mean \pm SD. **** $p < 0.0001$, *** $p < 0.001$, ** $p < 0.01$, * $p < 0.05$, ns no significance

granzyme B as well as downregulated markers of exhausted cells, such as PD1 and TIM3. More importantly, in vivo experiments showed that splenic CD8⁺ T cells matured after stimulation because the markers of naïve T cells were downregulated (CCR7 and TCF7) (Fig. 1t, u). In addition, the percentage of granzyme-B⁺ CD8⁺ T cells of VNP _{α TNF- α} group was increased in immune organs, particularly in tumor, which was four times higher than the control group (Fig. 1v). And VNP _{α TNF- α} stimulated more Ki67⁺ cytotoxic CD8⁺ T cell, which was five times higher than the control group (Fig. 1w). These results indicated that VNP _{α TNF- α} mobilized the systemic immune response. Furthermore, it is noteworthy that VNP _{α TNF- α} reduced CD8⁺ T cell death approximately two-fold (Supplementary Fig. S5f). Notably, the same results were previously reported that anti-TNF- α inhibitor lessened CD8⁺ T cell death in vivo.⁹ Meanwhile, CD8 Tregs were reduced in the tumor draining lymph nodes (TdLNs) and tumor after VNP _{α TNF- α} administration (Fig. 1x, Supplementary Fig. S5g, i). As expected, the percentage of Annexin V-positive CD8 Tregs was increased approximately twice after VNP _{α TNF- α} administration (Supplementary Fig. S5h), which means that the tumor immunosuppression was alleviated.

Based on our strategy, TNF- α nb could be delivered into tumor tissue by VNP safely and efficiently, and this system exerted robust antitumor effects with controllable TNF- α nb secretion in melanoma with only one dosage, which could also avoid the side effects and high costs of TNF- α inhibitors. Moreover, VNP _{α TNF- α} promoted antitumor immune responses in a melanoma tumor microenvironment by mobilizing tumor immune response as follows, (1) VNP _{α TNF- α} reduced tumor angiogenesis. (2) VNP _{α TNF- α} stimulated DCs maturation manifesting as elevated CD86. DCs activated CD8⁺ T cells by antigen-presentation and induced CD8⁺ T cells to upregulate Granzyme-B and Ki67, stimulated cytotoxic CD8⁺ T cell induced tumor apoptosis. (3) CD8 Treg reduced after administration of VNP _{α TNF- α} . (4) VNP _{α TNF- α} directly induced tumor apoptosis in vivo and in vitro (Fig. 1y). In addition, VNP _{α TNF- α} causes acceptable splenomegaly but has better biosafety than VNP (Supplementary Fig. S8a–f).

DATA AVAILABILITY

All data generated or analyzed during this study are included either in this article or in the supplementary information files.

ACKNOWLEDGEMENTS

This study was supported in part by grants from the National Natural Sciences Foundation of China (82130106, 32250016), Nanjing Special Fund for Life and Health Science and Technology (202110016, China), Changzhou Bureau of Science and

Technology (CJ20210024, CZ20210010, CJ20220019, China) and Jiangsu Target-Pharma Laboratories Inc., China.

AUTHOR CONTRIBUTIONS

Z.C.H. and Z.T.C. conceived the idea and designed the experiments, L.N.L. carried out most of the experiments, analyzed data, and wrote the original draft. X.L. designed partial experiments analyzed the data. W.J.X., L.L.Z., B.L.H. helped to analyze the data and provided valuable advice. C.H. provided laboratory assistance. All authors have read and approved the article.

ADDITIONAL INFORMATION

Supplementary information The online version contains supplementary material available at <https://doi.org/10.1038/s41392-023-01364-0>.

Competing interests: The authors declare no competing interests.

Consent for publication: All authors have agreed to publish this manuscript.

Ethics: All experimental procedures were approved by the Institutional Animal Care and Use Committee of the Nanjing University. (IACUC-2003167).

Lina Liu¹, Xing Liu¹, Wenjie Xin¹, Lulu Zhou², Baolian Huang²,
Chao Han¹, Zhiting Cao^{2✉} and Zichun Hua^{1,2,3✉}

¹The State Key Laboratory of Pharmaceutical Biotechnology, School of Life Sciences, Nanjing University, Nanjing 210023 Jiangsu, China;

²School of Biopharmacy, China Pharmaceutical University, Nanjing 210023 Jiangsu, China and ³Changzhou High-Tech Research Institute of Nanjing University and Jiangsu TargetPharma Laboratories Inc., Changzhou 213164 Jiangsu, China

Correspondence: Zhiting Cao (caozt@cpu.edu.cn) or Zichun Hua (zchua@nju.edu.cn)

REFERENCES

1. Segal, S. et al. Clinical signs, pathophysiology and management of cutaneous side effects of anti-tumor necrosis factor agents. *Am. J. Clin. Dermatol.* **18**, 771–787 (2017).
2. Harrison, M. L. et al. Tumor necrosis factor alpha as a new target for renal cell carcinoma: two sequential phase II trials of infliximab at standard and high dose. *J. Clin. Oncol.* **25**, 4542–4549 (2007).
3. Madhusudan, S. et al. Study of etanercept, a tumor necrosis factor-alpha inhibitor, in recurrent ovarian cancer. *J. Clin. Oncol.* **23**, 5950–5959 (2005).
4. Paik, P. K. et al. Phase I trial of the TNF-alpha inhibitor certolizumab plus chemotherapy in stage IV lung adenocarcinomas. *Nat. Commun.* **13**, 1–8 (2022).
5. Liang, K. et al. Genetically engineered *Salmonella typhimurium*: recent advances in cancer therapy. *Cancer Lett.* **448**, 168–181 (2019).
6. Xing, L. et al. Exogenous Annexin 1 inhibits Th17 cell differentiation induced by anti-TNF treatment via activating FPR2 in DSS-induced colitis. *Int. Immunopharmacol.* **107**, 108685 (2022).

7. Chen, A. Y. et al. TNF in the era of immune checkpoint inhibitors: friend or foe? *Nat. Rev. Rheumatol.* **17**, 213–223 (2021).
8. Wculek, S. K. et al. Dendritic cells in cancer immunology and immunotherapy. *Nat. Rev. Immunol.* **20**, 7–24 (2020).
9. Perez-Ruiz, E. et al. Prophylactic TNF blockade uncouples efficacy and toxicity in dual CTLA-4 and PD-1 immunotherapy. *Nature* **569**, 428–432 (2019).



Open Access This article is licensed under a Creative Commons Attribution 4.0 International License, which permits use, sharing, adaptation, distribution and reproduction in any medium or format, as long as you give

appropriate credit to the original author(s) and the source, provide a link to the Creative Commons license, and indicate if changes were made. The images or other third party material in this article are included in the article's Creative Commons license, unless indicated otherwise in a credit line to the material. If material is not included in the article's Creative Commons license and your intended use is not permitted by statutory regulation or exceeds the permitted use, you will need to obtain permission directly from the copyright holder. To view a copy of this license, visit <http://creativecommons.org/licenses/by/4.0/>.

© The Author(s) 2023